First results of inaugural deployments of the Australian National Ocean Bottom Seismograph Fleet

Alexey Goncharov*
Geoscience Australia
GPO Box 378 Canberra ACT 2601
alexey.goncharov@ga.gov.au

Ashby Cooper
University of Tasmania
20 Castray Esplanade, Battery Point TAS 7004
ashby.cooper@utas.edu.au

Peter Chia
Shell Australia
2 Victoria Avenue, Perth WA 6000
Peter.Chia@shell.com

Michal Malinowski
Institute of Geophysics, Polish Academy of Sciences
Księcia Janusza, 64, 01-452 Warsaw, Poland
michalm@igf.edu.pl

SUMMARY

The Australian National Ocean Bottom Seismograph Fleet is part of AuScope's Australian Geophysical Observing System (AGOS) - an initiative of the Australian Government funded through the Education Investment Fund. These instruments will greatly contribute to the understanding of the crust beneath oceanic basins surrounding Australia. In 2014-15 the Australian National OBS Fleet was utilised by the petroleum industry on a number of seismic surveys. High-quality data were recorded at all OBS deployment sites, often to offsets sufficiently large to detect Pn phases - refractions from the upper mantle. Analysis of earthquake data recorded during marine seismic surveys suggests strong interaction between anthropogenic signals (airgun source, vessel noise) and the natural environment, and allows arguing that in some instances earthquake energy contaminates marine reflection data in the frequency pass-band needed for petroleum exploration. Recording earthquake and airgun signals at fixed locations opens up a completely new possibility for calibration and comparison of those signal strengths and spectral compositions.

Key words: Ocean Bottom Seismographs, refraction, earthquake/airgun signal interaction.

INTRODUCTION

Coverage of the Australian Maritime Jurisdiction by deep penetrating seismic velocity measurements from existing refraction seismic studies is rather poor, and some parts of the Australian Antarctic Territory are better covered by such measurements (Fig. 1). The need to improve this was one of the drivers for the establishment of the Australian National Ocean Bottom Seismographs (OBS) Fleet. The other drivers were: (a) crustal thickness and composition are needed to constrain subsidence and hydrocarbon maturation modelling, and both of these are hard to get from reflection (streamer) data); and (b) better seismic velocities are needed for pre-stack depth migration and depth conversion of reflection data than those derived from streamer data, particularly in the deeper crust. OBSs are able to record passive source data (earthquakes, ambient noise) as well as active source (airgun generated) data. Passive seismic techniques are a cheaper way to obtain certain seismic information than marine reflection surveys, which is particularly attractive in the current low oil price environment.

In 2013 the Australian Government acquired 20 state-of-the-art broadband OBS units designed and built by Güralp Systems Ltd (UK). In 2014-15 the Australian National OBS Fleet was utilised by the petroleum industry on a number of seismic surveys (Fig. 2). High-quality data were recorded at all OBS deployment sites, often to offsets sufficiently large to detect possible Pn phases - refractions from the upper mantle. Such information means that the crustal thickness as well as the seismic velocity distribution to the Moho can be determined. As a result, these data can provide important constraints for subsidence and hydrocarbon maturation modelling. Analysis of earthquake energy recorded simultaneously with airgun signal has not been reported much (if ever) in the literature. The possible 'earthquake

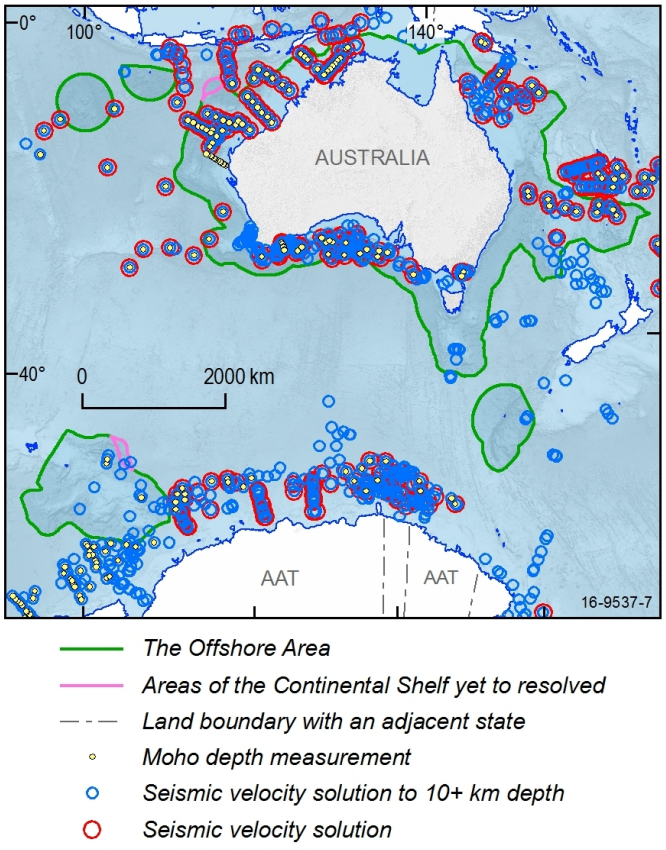

Figure 1: Refraction seismic velocity measurements, Australian Maritime Jurisdiction and Australian Antarctic Territory from Geoscience Australia database.

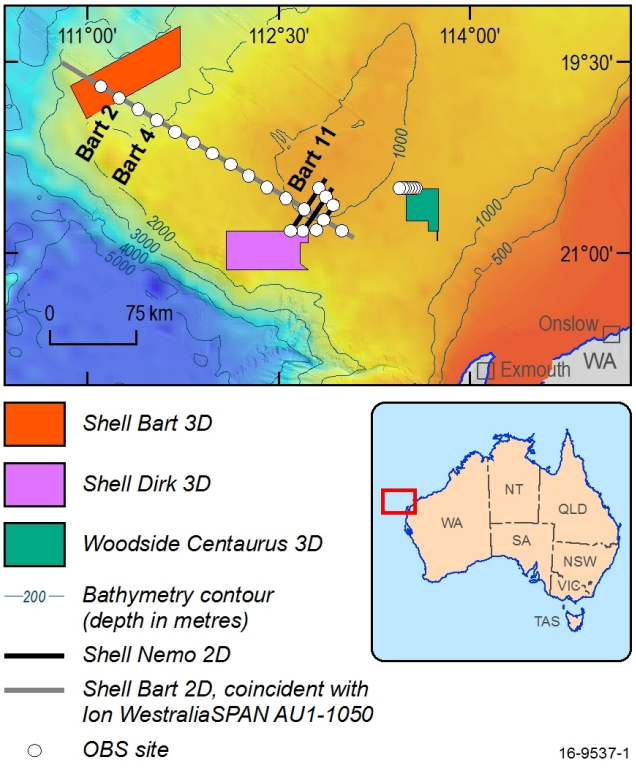

Figure 2: Location of the 2014-15 OBS deployments and marine reflection seismic surveys recorded by OBSs.

contamination' of marine reflection data in the frequency pass-band needed for petroleum exploration is an intriguing phenomenon and will be discussed further in this paper.

TECHNICAL SPECIFICATIONS OF AUSTRALIAN OBSs

The Güralp OBS is a broadband instrument with similar specifications to their land-based portable seismometers. Thus, passive seismic techniques developed for onshore studies can equally be applied to OBS surveys. Additionally, surveys utilising both onshore and offshore instruments are now possible. An OBS can remain on the seafloor continuously recording data for up to 12 months. Each OBS incorporates: (1) CMG-6T-OBS 3-component broadband (flat frequency response from 0.0167 Hz to 100 Hz) seismometer with a titanium housing; (2) hydrophone (flat frequency response from 1 Hz to 30 KHz) attached to the fourth channel of the digitiser; (3) high precision CMG Real Time clock with accuracy of better than a microsecond. The dimensions of each OBS are 1.30 X 0.72 X 0.75 m. Its weight is 236 kg (188 kg without concrete ballasts) in the air, whilst in water an OBS instrument in full assembly is negatively buoyant and weighs only 15 kg. Each instrument is capable of recording data on four channels with a maximum sampling frequency of 1000 samples per second (1 ms sampling rate). Data are recorded onto in-built flash memory and downloaded from the OBS upon recovery. After deployment, the instrument is acoustically pinged from several locations to establish its location and depth on the sea-floor through a triangulation procedure, similar to that used to locate earthquakes. The units are extremely versatile and can contribute valuable data relevant to many areas of geoscience, including passive seismology, ambient noise seismology, active source seismic experiments (in particular, marine seismic surveys) and environmental monitoring.

SHELL AUSTRALIA DAB OBS SURVEY

During the summer of 2014-2015, Shell Australia conducted the Dirk-Adventure-Bart (DAB), seismic survey over the Exmouth Plateau on the Australian NW margin. The survey consisted of three conventional 3D reflection surveys and four dedicated OBS 2D refraction lines (Fig. 2). The shooting interval for the 2D OBS refraction lines was 100m. This rather large, by marine reflection seismic standards, shot interval was defined on the basis of pre-survey modelling to minimise contamination of useful signal by noise from previous shots (Goncharov et al., 2016). The seismic airgun source utilised during the Shell DAB survey was an industry standard 4630 cubic inch broadband array, which is a much smaller volume array compared to what is commonly used for deep crustal OBS refraction studies. The dedicated OBS refraction lines consisted of: (1) 280 km long 2D OBS line, known as the BART 2D Line; (2) three, up to 55 km long 2D OBS lines, known as the NEMO 2D Lines (Fig. 2). In addition to this, two 3D OBS data subsets were recorded: (1) OBSs deployed at NW sites on BART 2D line (BART 1 – BART5) recorded shots from 4 lines of the BART 3D survey area; (2) OBSs deployed at sites BART 12, 13 and NEMO 1 – 6 recorded shots from 24 lines from the DIRK 3D survey. The OBS survey incorporated a total of 20 OBS deployments, with a maximum water depth of 2425 m. The instruments were deployed for an extended period of time of up to 47 days for some instruments used on the BART 2D line.

OBS units deployed during active source surveys will still record ambient signal from earthquakes and natural sources. For each OBS instrument within the Shell Australia DAB survey, the largest tele-seismic earthquakes occurring during the instrument deployment period were extracted from a total of 20 of such events occurring during the survey. This passive seismic data set is currently being analysed at Geoscience Australia and the University of Western Australia.

DISCUSSION

Active source data

The signal-noise ratio of an airgun generated signal at large offsets is very high, allowing recovery of information from very deep crustal features, in particular Moho refractions (Fig. 3). These refraction phases that can be tracked at some OBS sites to 100+ km offsets are critically important because they allow estimation of the velocity below the refractor, and to uniquely identify the bottom of the crust. This task is rather difficult on the basis of conventional reflection data, particularly if there is a number of competing distinct reflections in the deep section, as is the case on the coincident ION Westralia SPAN profile AU1-1050 (Bellingham and McDermott, 2014, p.58). The limited offset capability of streamer-based surveys means that these features are poorly imaged during conventional marine seismic acquisition. Thus, from the combined interpretation of reflection and refraction phases, OBS surveys

have the capability to image the velocity distribution of the whole crust. It has been shown that using *highly sensitive broadband* OBS units, even a relatively small volume broadband airgun array can provide enough energy at large (up to 100+ km in some cases) offsets to image the whole crust. For comparison, a 12000 cubic inch airgun array used for an OBS study of the Nankai Trough has not achieved consistent recording of the Moho refractions at offsets larger than 70 km (Operto et al., 2006). Also of note, is the comparison of data quality between the hydrophone and the vertical component of the seismometer. The hydrophone records considerably less information and appears to be more sensitive to water-born multiples than the seismometer (Fig. 3).

On the south-eastern extremity of the long BART 2D line, the orthogonal NEMO 2D lines (see Fig. 2) were acquired to provide high resolution refraction data from the mid to upper crust. The refraction data from these seismic lines show the same high-quality first arrival information as on the BART 2D line, with useful signal up to 55 km source-receiver offsets. All eight OBSs deployed at NEMO 2D lines, in addition to in-line recording, recorded large offset refraction data from adjacent 2D lines (i.e., off-line records) thus, allowing pseudo-3D (or 2.5D) data processing. Signal from 24 sail lines of the DIRK 3D reflection survey was also recorded at these eight sites, thus making this OBS data sub-set the most voluminous of all recorded so far.

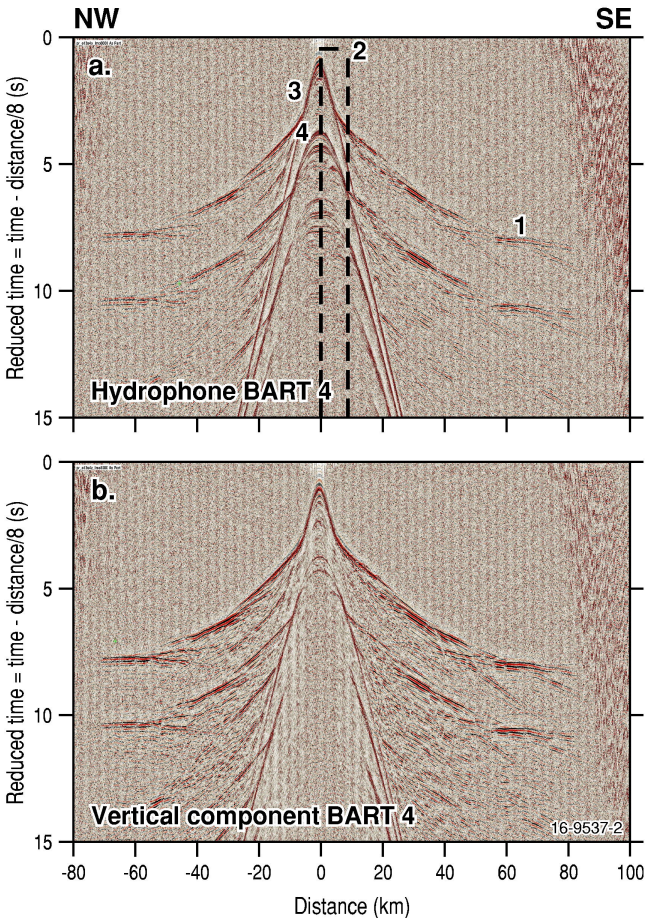

Figure 3: Common receiver gathers for vertical component seismometer and hydrophone at site BART 4 from the Shell BART 2D OBS line: 1 – possible Pn phases (refractions in the upper mantle) plot parallel to horizontal axes due to the reduced time scale; 2 – limits of offsets recorded in the multichannel reflection streamer data (shown to emphasize how much useful information is missing without recording at large offsets); 3 – direct water wave recorded as first arrivals at near offsets; 4 – first water wave multiple reflection. Note (a) high signal to noise ratio preserved to offsets in excess of 70km, (b) higher amplitude water multiples recorded on the hydrophone compared to the vertical seismometer, (c) considerably less useful phases immediately after the first arrivals in the hydrophone records than in the seismometer data.

First-pass 2D and 1D velocity-depth models from the BART 2D line show significant lateral velocity variation, particularly in the deeper crust, and point to substantial variation in Moho depth along the line. Velocity models will be refined as 2D interpretation progresses with the incorporation of subsequent arrivals (in particular, PMP reflections from the Moho).

Passive source data

The largest tele-seismic earthquakes recorded during the instrument deployment period were extracted from a total of 20 such events occurring during the survey. The events varied in magnitude from 5.6 to 6.6 MS. Further analysis of passive source data recorded during the active source survey is ongoing, and will provide new information on the suitability of these data for application of conventional passive source techniques (receiver function analysis, shear wave splitting, and others). Most of the earthquakes recorded during the Shell DAB survey were recorded at the time when the airgun signal was also being recorded. Recording earthquake and airgun signals at the same locations opens up a completely new possibility for calibration and comparison of those signal strengths and spectral compositions.

Earth – Ocean – Airgun signals interaction

Analysis of earthquake energy recorded simultaneously with airgun signal is a rather new research area and it is difficult to even suggest effective tools for such analysis. In this section we will be looking at the spectral characteristics of complex interfering signals (earthquake energy, airgun signal, ambient noise, shooting vessel noise, and, possibly, some other types of energy). Spectral characteristics of this complex 'interference mix' will be analysed in two types of time windows: long windows (~800 s) which we term 'seismology windows' because they are more targeted at spectral analysis of earthquake energy (Fig. 4), and much shorter windows (1 s), deemed 'seismic exploration windows', that are more targeted at airgun generated signal (Fig. 5). 'Seismology windows' include (Fig. 4), arguably, a more complicated 'interference mix' than 'seismic exploration windows', at least because they are indiscriminate to any type of airgun generated signal, be it first refracted arrivals, or reflections from sub-seafloor geological boundaries (P and S), converted phases or direct water waves, etc. 'Seismic exploration windows' are more discriminate: they are positioned either immediately before first airgun signal arrivals, or centred on first arrivals of airgun signal (Fig. 5), but they still include (although to a much lesser extent than 'seismology windows') some earthquake energy and

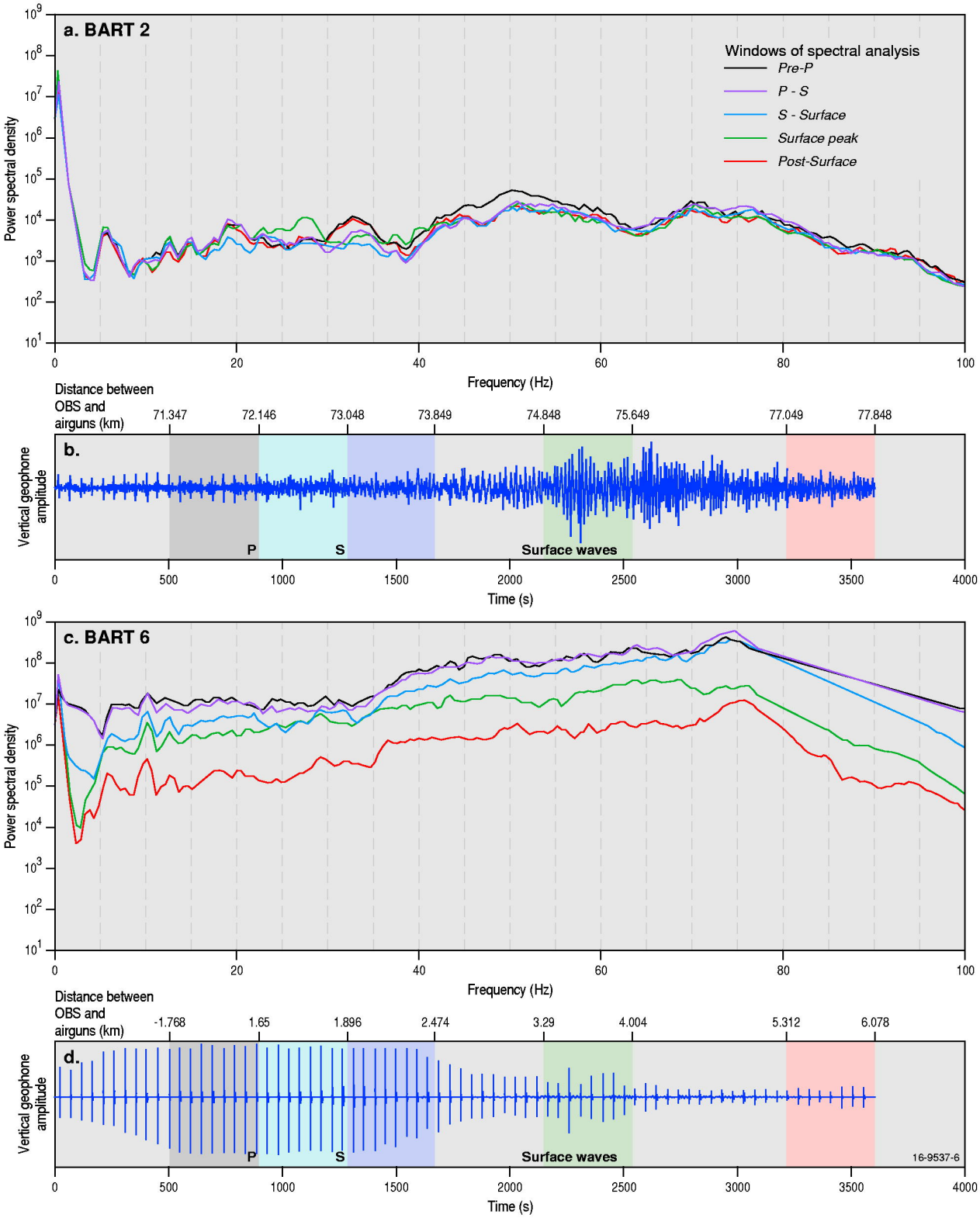

Figure 4: Power spectral density (a, c) and corresponding vertical geophone seismograms (b, d) from sites BART 2 and 6 around the estimated arrival time of the seismic waves from the magnitude 6.6 earthquake in the Solomon Islands. The beginning of the seismogram (0 s) is ~900 s before the estimated arrival time of the first P-waves from that earthquake. The estimated arrival times of P and S-waves from the earthquake are marked P and S respectively. The records show high-frequency and high-amplitude repetitive pulses from the airgun source, and lower frequency signals from the earthquake. Five windows of spectral analysis of different parts of seismogram are marked in (b) and (d) by different colours, and corresponding spectrograms in (a) and (c) are annotated in the legend. Note differences in distances between OBSs and airguns at the time of the earthquake energy arrival: from -1.768 km at the beginning of the first spectral analysis window at site BART 6 to 77.848 km at the end of the last spectral analysis window at site BART 2. Negative distances correspond to shooting vessel and airguns to the NW of OBS locations.

ambient noise. Unlike the case with 'seismology windows', spectral analysis in the 'seismic exploration windows' is undertaken on *discontinuous segments* of seismic traces extracted from original continuous records. The start time of these traces is based on individual airgun shot times as a trigger for the extraction of 30 s long traces. A number of 1 s long segments of those 30 s long traces are then combined together within a window that is ~5 km wide along the horizontal axis (Fig. 5). The power spectral densities presented in Fig. 5b correspond to the resulting *composite* traces. Investigating the interaction between these signals and noise is a complex task. In this paper we demonstrate one such method to quantify and compare the spectral and amplitude characteristics of the seismic wavefield. We put this topic forward for debate.

Signal from a magnitude 6.6 MS earthquake in the Solomon Islands was recorded at several sites during the Shell DAB survey. The earthquake signal is visible (Fig. 4b) as a longer period signal that lasts for the full trace length starting at the time of the P-wave arrival. The low-frequency high-amplitude signal observable on vertical component of the seismometer starting sometime after 1500 s mark is likely due to the presence of surface wave energy from the earthquake. At this time, airgun signal was also being recorded from the BART 2D line and is clearly identified by the regular short lived pulses with a high amplitude spike corresponding to the arrival of a water wave (Fig. 4b, d). Airgun signal dominates when the distance between the OBS and airguns is small. In this case earthquake energy is undetectable by visual inspection of the time series, such as the example from site BART 6 (Fig. 4b, d). The distance between the site BART 6 and airguns at the time of earthquake energy arrival was from ~ 2 to ~ 6 km (Fig. 4d). It is noticeable that the airgun signal amplitude decreases with increasing distance, and at site BART 2, when the distance between the OBS and airguns at the time of earthquake energy arrival is ~75 km, it becomes invisible to the background of surface waves from the earthquake (Fig 4b). Analysis of the spectral composition of vertical component seismogram at ~75 km distance between the OBS and airguns (Fig. 4a) shows a very prominent microseismic peak at low frequency values corresponding to periods of 6-7 s (Fabrice et al., 2015). This high amplitude feature has a rather narrow frequency range: its power spectral density at 3-4 Hz drops from peak values by ~5 orders of magnitude.

There is no detectable airgun signal contribution to the microseismic peak: the pre-P (black) curve in Fig. 4a corresponds to the part of the seismogram where airgun signal is recorded before the arrival of P-wave energy from the earthquake. The corresponding

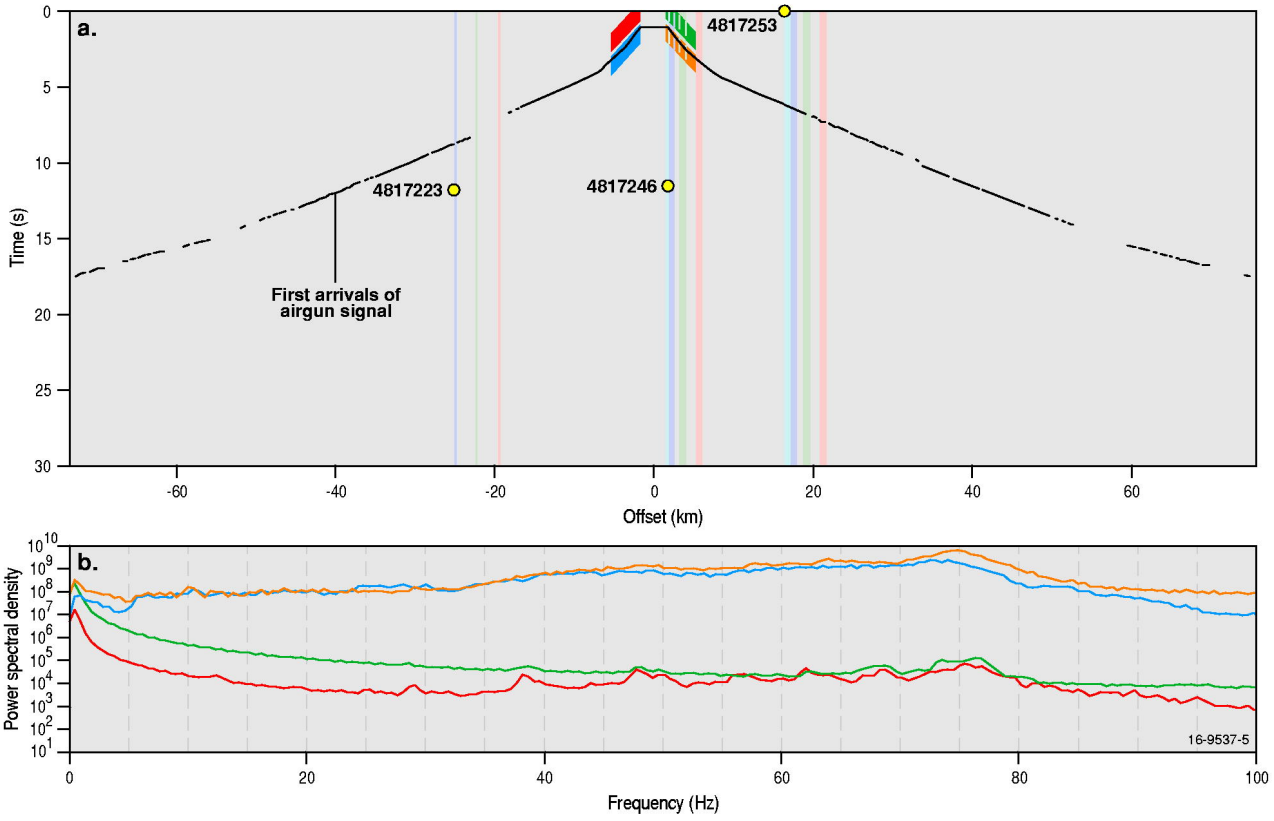

Figure 5: Travel times of first arrivals of airgun signal (a) and power spectral density within select analysis windows (b) at site BART 6. Long spectral analysis windows of different parts of earthquake seismograms (as those in Fig. 4) are marked in (a) and colour coded identical to Fig. 4. Yellow dots – estimated arrival times of the P-wave energy from earthquakes with catalogue IDs of earthquakes labelled. ID 4817246 corresponds to Solomon Islands earthquake illustrated in Fig. 4. Two pairs of short spectral analysis windows are shown as parallelograms on each side of OBS location: one window in each pair is positioned immediately before airgun signal arrivals, and the other one centred on first arrivals of airgun signal. Spectral charts in (b) are colour coded identical to short windows' colours in (a).

power spectral density curve is indistinguishable from those corresponding to other spectral windows within the microseismic passband. From 3-4 Hz and above the airgun signal contribution becomes noticeable. The Pre-P (that is ambient noise *plus airgun*

signal, but no earthquake signal contribution) power spectral density at ~50 Hz is ~2 orders of magnitude greater than that at 3-4Hz. Interestingly, the frequency range of 40 to 60 Hz is the only spectral domain where airgun signal has a power spectral density greater than any of the other spectral analysis windows of Fig. 4 (a, b). With some simplification, it can be concluded that within the frequency range from 3-4 to ~40 Hz the earthquake signal contributes enough energy for the resulting interference signal (earthquake plus airguns) to have higher power spectral density than that in the pre-P spectral analysis window (airguns and ambient noise only, but no earthquake contribution).

The power spectral density distribution changes radically when interfering airgun and earthquake signals are recorded at OBS locations close to the airguns at the time of earthquake energy arrival (Fig. 4c). At station BART 6, earthquake energy from the Solomon Islands event arrives when the shooting vessel is only 1.6 to ~4.0 km away (Fig. 4d). First, it should be noted that the airguns contribute up to 5 orders of magnitude to the power spectral density curve between ~10 and ~100 Hz (from comparison between the pre-P (black) curves in Figs. 4a and 4c). Second, as the pre-P (black) curve in Fig. 4c shows, the power spectral density drop from the microseismic peak to its magnitude at 3-4 Hz is only ~1 order of magnitude, compared to ~5 orders of magnitude at site BART 2 (Fig. 4a). We conclude that *non-earthquake* energy contribution at small OBS-airguns offsets (less than ±2 km, see pre-P, grey window location in Fig. 4d) is strong enough to *almost* close the spectral gap between the microseismic peak (less than 0.5 Hz) and the nominal airgun signal (from 5 Hz and above). There is a possibility that this *non-earthquake* energy is one of, or a combination of: airgun generated signal (although the nominal flat signature of broadband airgun array on Shell DAB survey was modelled to be from 5 to 90 Hz), shooting vessel noise, and/or noise generated by an array of ten 10-km long streamers towed behind the seismic vessel. Further research is needed to quantify the relative contributions from these multiple sources to the complex 'interference mix', and to understand better the effects of *non-airgun* generated energy on reflection seismic data recorded on streamers in a very low (0.5 – 5.0 Hz) frequency range.

Results of spectral analysis within the short, 'seismic exploration windows' (Fig. 5), allow separation of airgun and non-airgun energy contributions to the resulting interference signal. However, we have so far undertaken only a limited analysis of this type. Results presented below are based on the data from only one site BART 6, and therefore cannot be treated as conclusive.

First, comparison of the power spectral density curve within the two (red and blue) analysis windows located to the NW (left) of the OBS suggests that airgun signal contribution (rather than vessel or streamer array noise) at these small OBS-airguns offsets is responsible for closing the spectral gap between ~0.5 and ~5.0 Hz described above. This is because the *pre-first arrivals* spectral density curve (red-curve and red spectral window) in Fig. 5b shows a substantial (~2 orders of magnitude) drop between the microseismic peak values and those at ~5 Hz. Vessel and streamer array noise is present in this spectral analysis window, but does not appear to be strong enough to close the ~0.5-5.0 Hz gap. The power spectral density drop between the microseismic peak and ~5 Hz values is much less pronounced when the airgun generated signal is included in the analysis window (blue curve). Second, comparison of power spectral densities within the two (green and orange) analysis windows located to the SE (right) of OBS is consistent with these conclusions. Third, both spectral analysis windows located to the SE (right) of OBS include energy from the Solomon Islands earthquake (ID 4817246). Surprisingly, this energy appears to make a noticeable contribution not only near the microseismic peak frequencies (~0.5 Hz or less), but also up to frequencies as high as 50 to 60 Hz. This is very clear from the comparison of power spectral density curves (red and green in Fig. 5b) corresponding to *pre-first airgun arrivals* windows. Generally, Australia has very low seismic attenuation and local earthquakes have a high frequency content (to at least 200 Hz). Perhaps, such a high frequency content may also be found from waves that travel up the slab from earthquakes along the plate boundary (M. Salmon, pers. comm., 2016), as it may be the case for the Solomon Islands earthquake.

Finally, and perhaps most importantly for petroleum exploration oriented seismic surveys, there is a noticeable difference between power spectral densities within the analysis windows centred on the first airgun signal arrivals (blue and orange windows and spectral curves in Fig. 5). Spectral densities calculated to the SE (right) of the OBS location appear to be up to 10 times higher in the frequency range 0.5 to 5.0 Hz. We attribute this effect to the earthquake energy added to the airgun signal energy when the analysis window is to the SE (right) of the OBS location.

Ongoing analysis at other OBS sites (e.g., BART 4) suggests that under certain conditions seismic vessel noise and/or noise produced by an array of streamers towed behind the vessel produce spectral effects similar to the ones attributed to the energy of the Solomon Islands earthquake discussed above. Australian OBS data from the Shell DAB survey are a unique data set by global standards that allows further advancing the research in this poorly explored field.

CONCLUSIONS

OBS data collected during commercial seismic surveys in Australian territorial waters in 2014-15 prove the possibility to image whole crust and upper mantle velocity distributions and unequivocally define the Moho boundary from analysis of both reflected and refracted phases generated by an industry standard broadband airgun array and recorded at large (tens km) offsets. This means that valuable pre-competitive information on a regional scale can be obtained as a 'side effect' of commercial seismic surveys.

Analysis of passive source data recorded from 20 sufficiently strong earthquakes during active source surveys is ongoing, and will provide new information on these data suitability for application of conventional passive source techniques. Passive seismic techniques are a cheaper way to obtain certain seismic information than marine reflection surveys, which is particularly attractive in the current low oil price environment.

Recording earthquake and airgun signals at the same locations opens up a completely new possibility for calibration and comparison of those signal strengths and spectral compositions.

Analysis of earthquake data recorded during marine seismic surveys suggests strong interaction between anthropogenic signals (airgun source, vessel noise) and the natural environment, and allows arguing that in some instances earthquake energy contaminates marine reflection data in the frequency pass-band needed for petroleum exploration. Further analysis of the interference of active and passive source signals of different types is needed to shed new light on this poorly understood problem.

ACKNOWLEDGMENTS

Ray de Graaf, Wayne Peck, Andrew Latimore, Craig Wintle, Dejvid Aleksovski, Stephen Hodgkin, as the Australian OBS Team, made an outstanding contribution to the establishment of the ocean bottom seismography in Australia. Richard Blewett and Tristan Kemp strongly supported establishment of the Australian OBS capability at Geoscience Australia. David Lumley (University of Western Australia) contributed to OBS surveys design and pre-survey modelling. Adam Pascale and Simon Heyes (ESS Earth Sciences) provided essential logistical and administrative support for those surveys. David Arnold produced final figures for this abstract; Ross Costelloe, Tristan Kemp and Murray Richardson peer reviewed it. Alexey Goncharov publishes with permission of the CEO, Geoscience Australia and Shell Australia. The Geoscience Australia GeoCat number for this publication is 90079.

REFERENCES

Bellingham, P. and McDermott, K., 2014. The Australian North West Shelf: New insights from Deep Seismic. GeoExPro, 11, 6, 57-62.

Fabrice, A., Gualtieri, L. and Stutzmann, E, 2015. How ocean waves rock the Earth: two mechanisms explain seismic noise with periods 3 to 300 s. Geophysical Research Letters, 2015, 42 (3), p. 765-772.

Goncharov, A., Cooper, A., Chia, P. and O'Neil, P., 2016. A new dawn for Australian ocean-bottom seismography, The Leading Edge, January 2016, v. 35, p. 99-104, doi:10.1190/tle35010099.1.

Operto,S., Virieux, J., Dessa J.-X.,and Pascal, G.,2006. Crustal Seismic Imaging from Multifold Ocean Bottom Seismometer Data by Frequency Domain Full Waveform Tomography: Application to The Eastern Nankai Trough. Journal of Geophysical Research, 111, B09306, doi:10.1029/2005JB003835.